



## Aberrant rich club organization in patients with obsessive-compulsive disorder and their unaffected first-degree relatives

Ziwen Peng<sup>a,\*</sup>, Xinyi Yang<sup>a,1</sup>, Chuanyong Xu<sup>a,1</sup>, Xiangshu Wu<sup>a</sup>, Qiong Yang<sup>b,c</sup>, Zhen Wei<sup>d</sup>, Zihan Zhou<sup>a</sup>, Tom Verguts<sup>e</sup>, Qi Chen<sup>a,\*</sup>

<sup>a</sup> Key Laboratory of Brain, Cognition and Education Sciences, Ministry of Education China, School of Psychology, Center for Studies of Psychological Application, And Guangdong Key Laboratory of Mental Health and Cognitive Science, South China Normal University, China

<sup>b</sup> Southern Medical University, Guangzhou, China

<sup>c</sup> Affiliated Brain Hospital of Guangzhou Medical University, Guangzhou, China

<sup>d</sup> Department of Child Psychiatry and Rehabilitation, Affiliated Shenzhen Maternity & Child Healthcare Hospital, Southern Medical University, Shenzhen, China

<sup>e</sup> Department of Experimental Psychology, Ghent University, Ghent, Belgium

### ARTICLE INFO

#### Keywords:

Obsessive-compulsive disorder  
Vulnerability  
Rich club organization  
Peripheral connections  
Diffusion tensor imaging

### ABSTRACT

Recent studies suggested that the rich club organization promoting global brain communication and integration of information, may be abnormally increased in obsessive-compulsive disorder (OCD). However, the structural and functional basis of this organization is still not very clear. Given the heritability of OCD, as suggested by previous family-based studies, we hypothesize that aberrant rich club organization may be a trait marker for OCD. In the present study, 32 patients with OCD, 30 unaffected first-degree relatives (FDR) and 32 healthy controls (HC) underwent diffusion tensor imaging (DTI) and functional magnetic resonance imaging (fMRI). We examined the structural rich club organization and its interrelationship with functional coupling. Our results showed that rich club and peripheral connection strength in patients with OCD was lower than in HC, while it was intermediate in FDR. Finally, the coupling between structural and functional connections of the rich club, was decreased in FDR but not in OCD relative to HC, which suggests a buffering mechanism of brain functions in FDR. Overall, our findings suggest that alteration of the rich club organization may reflect a vulnerability biomarker for OCD, possibly buffered by structural and functional coupling of the rich club.

### 1. Introduction

Obsessive-compulsive disorder (OCD) is a severe mental illness that seriously affects an individual's learning and working ability and social function, with intrusive thoughts and repetitive behaviors as main clinical manifestations (Robbins et al., 2019). This chronic and disabling illness is surprisingly frequent (2.5%–3%) in the general population (Robbins et al., 2019). However, the specific pathological mechanism of OCD is still unclear. Research on the brain structure and function of OCD is helpful for clarifying its pathomechanism and diagnosis.

The human brain can be considered as a highly complex network, formed by hundreds of brain regions and thousands of interconnected white matter (WM) axonal pathways (Cao et al., 2020; Sporns, 2011). In this view, brain function derives from the topology of the whole network, known as the brain connectome, rather than from individual

regions or connections (Bullmore and Sporns, 2009; Sporns et al., 2005). In addition, highly connected brain regions are said to be of high degree, or said to be “rich” (Sporns et al., 2007; van den Heuvel et al., 2010; van den Heuvel and Sporns, 2011). The rich club phenomenon is characterized by denser connectivity among rich club nodes than among nodes of lower degree. Rich club connections are thought to be crucial for promoting global information integration (van den Heuvel and Sporns, 2011). Connections between rich club and other nodes will be called feeder connections; connections among other (non-rich club) nodes will be called local connections.

Disruptions within rich club organization in psychiatric disorders have been reported in several studies, such as schizophrenia (van den Heuvel et al., 2013), Alzheimer's disease (Cao et al., 2020; Lee et al., 2018; Yan et al., 2018), bipolar disorder (Wang et al., 2018; Zhang et al., 2018), attention-deficit hyperactivity disorder (Wang et al., 2019) and

\* Corresponding authors at: School of Psychology, South China Normal University, No. 55, West of Zhongshan Avenue, Guangzhou 510631, China.

E-mail addresses: [pengzw@m.scnu.edu.cn](mailto:pengzw@m.scnu.edu.cn) (Z. Peng), [chen.qi@m.scnu.edu.cn](mailto:chen.qi@m.scnu.edu.cn) (Q. Chen).

<sup>1</sup> These authors contributed equally as first authors to this project.

<https://doi.org/10.1016/j.nicl.2021.102808>

Received 22 April 2021; Received in revised form 23 August 2021; Accepted 24 August 2021

Available online 2 September 2021

2213-1582/© 2021 The Author(s).

Published by Elsevier Inc.

This is an open access article under the CC BY-NC-ND license

(<http://creativecommons.org/licenses/by-nc-nd/4.0/>).

major depression disorder (Liu et al., 2020). White matter microstructure provides the structural backbone of the human brain; it underlies the brain's cognitive functions, and its alterations contribute to the neurobiological basis of OCD (Hu et al., 2020). It is therefore important to examine the rich club organization in the white matter brain network of OCD.

However, very few studies investigated the rich club organization in OCD. One previous study from Zhou et al. (2020) reported that the structural connectivity was increased not only among the rich club, but also among peripheral nodes, in OCD relative to HC. However, its functional counterpart remains unclear. Measuring the relationship between the structural and functional network, can reveal the functional consistency of the brain from the perspective of structural topology. This may allow detecting subtle neural changes more sensitively than with any single imaging modality (Greicius et al., 2009; Honey et al., 2009; Zhang et al., 2011b). Aberrant intrinsic functional connectivity (FC) (Cui et al., 2020; Fajnerova et al., 2020; Stern et al., 2012; Zhang et al., 2011a) and structural connectivity (SC) (Banks et al., 2015; Reess et al., 2016) between large-scale brain networks have both been reported in OCD. Both may cause cognitive impairment (Wang et al., 2014). But it remains unclear whether OCD patients also have disrupted coupling between SC and FC in the rich-club organization. This would be important because SC-FC consistency is a relatively direct indicator of the consistency between brain structure and function.

Family-based studies have demonstrated that the unaffected first-degree relatives (FDR) of OCD patients have 3–12 times more risk of developing OCD (Hanna et al., 2002; Nestadt et al., 2000; Pauls et al., 1995), suggesting a genetic predisposition in OCD. However, as the genetic basis for OCD remains unclear, some researchers have focused their efforts on examining the alterations in the unaffected sibling of individuals with OCD, which can provide genetic information for OCD research and help to disentangle the state and trait markers of the disorder (Peng et al., 2014a). Previous researches found that the (functional) hypoconnectivity in frontal-striatal areas in both patients and their clinically asymptomatic relatives may serve as a biomarker for OCD (Vaghi et al., 2017; Chamberlain et al., 2008). Moreover, previous neuroimaging studies have revealed network abnormalities, such as atypical small-world properties (Peng et al., 2013) and altered white matter (Menzies et al., 2008; Dikmeer et al., 2021), in both OCD patients and their FDR. However, whether the basis for information dissemination in those brain networks, namely the rich club, can be treated as a putative vulnerability biomarker, remains unknown. Such knowledge could deepen the understanding of the brain network of OCD at the mesoscale level.

To address this issue, we currently investigate the characteristics of rich club organization and explore whether rich club organization is a potential vulnerability biomarker of OCD. We performed diffusion tensor imaging (DTI), which is a frequently used and noninvasive technique to probe the WM microstructure and to reveal structural network information in the human brain (Cao et al., 2020; Jbabdi et al., 2015). The relationship between rich club connectivity and diagnosis, and between rich club connectivity and OCD symptomatology was also examined to explore how structural network changes contribute to OCD. Finally, resting-state fMRI was used to construct the functional connections to detect the coupling between the functional and structural networks. In all, we investigated four hypotheses in this study. First, we investigated if OCD patients exhibited aberrant rich club organization or abnormal feeder and local connections. The second hypothesis was whether FDR showed a similar structural network alteration as patients. The third was whether the abnormal rich club organization in patients correlated with clinical characteristics. The fourth was whether the coupling between structure and function is changed in OCD patients and their FDR.

## 2. Methods

### 2.1. Participants

We recruited thirty-two OCD patients (males = 20, females = 12; for treatment details see [Supplementary materials](#)), thirty unaffected first-degree relatives (males = 18, females = 12) and thirty-two healthy controls (HC) (males = 18, females = 14) in Guangzhou Psychiatric Hospital and outside the hospital. All patients satisfied the Diagnostic and Statistical Manual of Mental Disorders, 4th edition (DSM-IV) criteria for OCD by applying the Structured Clinical Interview (SCID) for DSM-IV-TR Axis I disorders (First et al., 2002). Patients were excluded: (a) if they were younger than 18 or older than 55; (b) if they had a history of brain trauma or neurological disease; (c) if they had shown alcohol or substance abuse within 12 months prior to participating in this study. The FDR and HC were also screened for DSM-IV-TR Axis I disorders, and HC or their families with a history of any psychiatry disorders in DSM-IV were excluded.

Written informed consent was provided by all subjects after a detailed description of the study. The study was approved by the institutional research and ethics committee of Guangzhou Psychiatric Hospital.

### 2.2. Clinical assessments

The Yale-Brown Obsessive-Compulsive Scale (Y-BOCS) (Goodman et al., 1989) was used to estimate the illness severity. We used the Obsessive-Compulsive Inventory-Revised (OCI-R) (First et al., 2002; Peng et al., 2011) to characterize the specific categories of OCD symptoms, including obsessing, washing, neutralizing, checking, ordering, and hoarding. The Beck Depression Inventory (BDI) (Beck and Steer, 1984) was administered to assess depressive symptoms, and the State-Trait Anxiety Inventory (STAI) (Spielberger, 1983) to assess anxiety symptoms. We conducted ANOVA and chi-square tests in Statistical Package for Social Science (SPSS, version 23.0) (<https://www.spss.com>).

### 2.3. Imaging acquisition

The DTI and resting-state fMRI data were acquired on a 3.0-Tesla MR system (Philips Medical System, Netherlands) equipped with an eight-channel phased-array head coil by a skilled radiological technician. Echo Planar Imaging (EPI) sequences were applied to collect the resting-state fMRI data with the following parameters: time repetition (TR) = 2000 ms; echo time (TE) = 30 ms; flip angle = 90°, 33 slices, matrix = 64 × 64; slice thickness = 4.0 mm. For each participant, the fMRI scanning lasted for 480 s, and 240 volumes were obtained. During the scanning, participants were instructed to relax with eyes closed, and stay awake without moving. DTI data was collected with the following parameters: TR = 6000 ms; TE = 70 ms; flip angle = 90°, 50 slices; matrix = 128 × 128, slice thickness = 3 mm; 32b-value = 1000 s/mm<sup>2</sup>, 1b-value = 0. To spatially normalize and localize better, a high-resolution T1-weighted anatomical image was obtained using a magnetization prepared gradient echo sequence with the following parameters: TR = 8 ms, TE = 3.7 ms, flip angle = 7°, matrix = 256 × 256, and slice thickness = 1 mm.

### 2.4. DTI preprocessing and structural networks construction

The DTI processing was done using the Pipeline for Analyzing brain Diffusion images (PANDA) toolbox (Cui et al., 2013), which provides a convenient interface to invoke the functions from the FMRIB Software Library (Smith et al., 2004) (FSL, version 5.0.9), Diffusion Toolkit (DTK) (Wang et al., 2007) and TrackVis (Irimia et al., 2012). At first, DTI data was preprocessed including these steps: correction of eddy current distortion and head motion, skull stripping, and calculation of diffusion

tensor metrics including fractional anisotropy (FA). The skull of subjects' T1 data was stripped for better transforming the images in MNI space to individual native space later.

Then, deterministic fiber tracking (Mori et al., 1999) was carried out to reconstruct the whole brain fibers, using the Fiber Assignment by Continuous Tracking (FACT) algorithm. If the angle between the current and the previous streamline was greater than  $45^\circ$  (Li et al., 2013) or the FA value smaller than 0.2 (Koh et al., 2020), the current streamline tracking procedure was terminated. The orientation patch was achieved by inverting the Z component of the vector. After the fiber was tracked, the  $90 \times 90$  network matrix of each subject was calculated. The nodes of the network were defined by the 90 cortical and subcortical regions with the automated anatomical labeling (AAL) atlas (Tzourio-Mazoyer et al., 2002), which was transformed from MNI space to individual diffusion space for the parcellation of each subject's brain. The edge between two nodes was defined to be the number of fibers between that pair; fiber numbers (FN) lower than 2 were set as 0 to exclude spurious edges. Thus, we obtained the FN-weighted network matrix for structural analysis (Wang et al., 2019). We also carried out the analysis with thresholds 3 and 4, which led to very similar results (see Supplementary material, Fig. S3).

### 2.5. Rich club organization analysis

A rich club organization of a network means that the high-degree ( $k$ , the number of edges connected with a node) nodes of a network, connect more densely to each other than they connect to the nodes with a lower degree (Colizza et al., 2006). Formally, rich club organization was examined by the weighted rich-club coefficient  $\Phi^w(k) = \frac{2E_{>k}}{N_k(N_k-1)}$ , which is computed as the ratio of connections or edges ( $E$ ) between the nodes ( $N_1 \sim N_{90}$ ) with a degree  $> k$  and the total number of possible connections (van den Heuvel and Sporns, 2011; van den Heuvel et al., 2013). The rich club phenomenon is identified via a normalized coefficient  $\Phi^w \text{norm}(k) = \Phi / \Phi_{\text{random}}$ . The coefficient  $\Phi_{\text{random}}$  was computed the same as  $\Phi^w(k)$  but in a random network, created by randomizing the connections of the structural network, keeping the  $k$  distribution and sequence of the network matrix intact (Rubinov and Sporns, 2010). If the ratio is larger than 1 over a range of  $k$  (Colizza et al., 2006; van den Heuvel et al., 2013), the network is said to have the rich club property. We computed the weighted rich club coefficient  $\Phi^w(k)$  and the normalized rich club coefficient  $\Phi^w \text{norm}(k)$ . The rich club organization analyses were performed using MATLAB-based GREYNA (<https://www.nitrc.org/projects/gretna>) (Wang et al., 2015), and displayed with BrainNet Viewer (<https://www.nitrc.org/projects/bnv/>) (Xia et al., 2013). We constructed the group-averaged FN-weighted structural networks for the OCD, FDR, and HC, respectively. The rich club nodes were selected on the group level, defined as the top 9 (10%) highest degree in the brain consistently observed across all groups of subjects. The same analysis was conducted for rich club nodes defined as the top 8% (Tuladhar et al., 2017) and 12% (van den Heuvel et al., 2013; Collin et al., 2014) highest degree nodes, yielding very similar results (see Supplementary material, Fig. S2).

Three kinds of connections could be defined after dividing the brain regions into rich club and non-rich club nodes: Rich club connections between rich club nodes, feeder connections linking rich club nodes and non-rich club nodes, and local connections between non-rich club nodes (van den Heuvel et al., 2013; Wang et al., 2018). To examine the three types of connections in the whole brain, connection strength was calculated for each of the three types (Li et al., 2019; Sa de Almeida et al., 2021). The Rich-club connection strength is equivalent to the sum of reconstructed fibers between rich club nodes (Collin et al., 2014). Feeder connection strength was the sum of reconstructed fibers between rich club and non-rich club nodes; local connection strength was the sum of reconstructed fibers among non-rich club nodes. For each subject, we also examined overall connectivity strength (i.e., across all 90 nodes), to

provide information on global organization (Collin et al., 2014).

### 2.6. Functional image preprocessing and functional network construction

The Statistical Parametric Mapping toolbox (SPM 12, <https://www.filion.ucl.ac.uk/spm>) and Data Processing Assistant for Resting-State fMRI (DPARSFA version 4.4, <https://rfmri.org/dpabi>) were used to preprocess the fMRI data (Yan et al., 2016). Image preprocessing involves: 1) slice timing correction; 2) head motion correction, realignment, coregistration with the corresponding T1-volume; 3) nuisance covariate regression (24 head motion parameters, white matter signal and cerebrospinal fluid signal) (Friston et al., 1996); 4) spatial normalization into the stereotaxic space of the Montreal Neurological Institute and resampling at  $3 \times 3 \times 3 \text{ mm}^3$ ; 5) spatial smoothing with a 6-mm full-width half-maximum isotropic Gaussian kernel; 6) band-pass filtering (0.01–0.08 Hz); 7) micro-head-motion correction (scrubbing) according to frame-wise displacement (FD, Power) (Power et al., 2012) by replacing the rest-fMRI volume with FD  $> 0.5 \text{ mm}$  using nearest-neighbor interpolation method (cubic spline).

We then obtained an FC matrix with 90 nodes from the AAL atlas. The level of functional connectivity between each pair of nodes was computed as the Pearson correlation ( $r$ ) between their averaged blood-oxygen level dependent (BOLD) time series. The  $r$  values were subsequently normalized by Fisher Z transformation ( $Z = 0.5 \times \ln((1+r)/(1-r))$ ) to define the edges in the FC matrix. Negative correlation coefficients were converted to an absolute value (FC weighted network).

### 2.7. SC-FC coupling analysis

To evaluate the relationship between structural and functional alteration, a coupling analysis was performed on the SC and FC, for each kind of connection (rich club, feeder and local) and for the whole brain network. For the nonzero edges in both the SC and FC weighted matrix, we extracted and resampled the fiber numbers of the SC matrix into a Gaussian distribution (Honey et al., 2009). We then correlated the structural and functional connection strength values of each subject (van den Heuvel et al., 2013). Therefore, four different types of SC-FC coupling coefficients were obtained: correlation analyses of whole brain structural and functional connections; and similar correlations for the rich club, feeder and local connections.

### 2.8. Statistical analysis

We applied ANOVA to test group differences in age and education, while a chi-square test was used to determine the gender difference among groups. The group differences in rich club organization parameters ( $\Phi^w \text{norm}(k)$ , rich club strength, feeder strength, and local strength) and SC-FC coupling value were further tested by an analysis of covariance (ANCOVA), controlling for age, gender, years of education, anxiety and depression levels. Moreover, post hoc tests were performed after the comparison of rich club organization using the Bonferroni correction for multiple comparisons. For the relationship between rich club organization and clinical variables, Pearson correlations were calculated in the OCD group with age, gender, education, anxiety, depression levels and disease duration being controlled. Finally, the relationship between each kind of connection strength and OCD diagnosis across all subjects, two dimensions of OCD symptom (obsession or compulsion) was determined applying 6 multivariate regression models, with age, gender, education, anxiety and depression levels being controlled, all with the following structure: Connection strength  $\sim$  OCD diagnosis + symptom + covariates. Because diagnosis and symptom were not on the same measurement scale, their individual data were mean-centered across subjects. Significance level was set at  $P < 0.05$  (uncorrected). Supplementary material (Figs. S5 and S6) presents other global network measures, group comparison, and correlation analyses.

### 3. Results

#### 3.1. Demographic and clinical variables

Table 1 displays the demographic and clinical characteristics of all participants. No significant difference was found in age ( $p = 0.185$ ), gender ( $p = 0.877$ ), and years of education ( $p = 0.830$ ) among OCD patients, FDR and HC subjects. The mean and standard deviation of total Y-BOCS scores were  $26.59 \pm 4.89$  in the OCD patients; the Y-BOCS obsession and compulsion scores were  $15.31 \pm 2.93$  and  $11.28 \pm 4.86$ , respectively. Moreover, for the scores of both STAI and BDI, significant differences among the three groups were observed ( $p < 0.001$ ); both the scores of STAI and BDI in OCD patients were significantly higher than in HC (STAI-state:  $p = 0.002$ , STAI-trait:  $p = 0.005$ , BDI:  $p < 0.001$ ), and significantly higher than in FDR (STAI-state:  $p < 0.001$ , STAI-trait:  $p < 0.001$ , BDI:  $p < 0.001$ ).

OCD, Obsessive-compulsive disorder patients; FDR, First-degree relatives; HC, Healthy comparison subjects; Y-BOCS, Yale-Brown Obsessive-Compulsive Scale; OCI-R, Obsessive-Compulsive Inventory-Revised; STAI, State-Trait Anxiety Inventory; BDI, Beck Depression Inventory; SD, Standard Derivation.

#### 3.2. Rich club organization

The average rich club coefficient of OCD, FDR and HC groups, are displayed in Fig. 1A. For all three groups of subjects, a normalized rich club coefficient ( $\Phi_{\text{norm}}^w$  greater than 1) was observed over a range of thresholds  $k = 1-12$ , indicative of a rich-club property in each group (Van den Heuvel et al., 2013). The ANOVA reveals that there were no significant differences among the groups except at  $k = 5$  ( $p = 0.018$ ) and  $7$  ( $p = 0.006$ ). We found 9 rich club regions in the structural networks, namely right putamen (PUT.R), bilateral precentral gyrus (PreCG.L, PreCG.R), bilateral supplementary motor area (SMA.L, SMA.R), bilateral precuneus (PCUN.L, PCUN.R), left postcentral gyrus (PoCG.L) and left temporal middle gyrus (MTG.L) (Fig. 1B). More details for each group on the rich club organization can be found in Supplementary material (Fig. S1).

The ANCOVA reveals significant differences in the connection strength of overall ( $p < 0.001$ ), rich club ( $p = 0.026$ ), feeder ( $p = 0.001$ ) and local connections ( $p < 0.001$ ) among all groups (Fig. 1C). On the overall connection strength, we found a significant ordered difference which means that a higher overall strength in HC than in FDR ( $p = 0.019$ ) and than in OCD ( $p < 0.001$ ) was found, and overall strength was also higher in FDR than in OCD ( $p = 0.046$ ). Compared with HC, OCD presented a decreased rich club ( $p = 0.008$ ), feeder ( $p < 0.001$ ) and local ( $p < 0.001$ ) connection strength. We also found an increase in feeder connection of FDR when compared to patients. Finally, in local connection strength, a significant decrease was observed in OCD relative to HC ( $p = 0.017$ ).

**Table 1**  
Demographic and clinical characteristics.

Variables	OCD (n = 32) (M $\pm$ SD)	FDR (n = 30) (M $\pm$ SD)	HC (n = 32) (M $\pm$ SD)	F/x2	p value
<i>Demographic Measures</i>					
Age, years	29.66 $\pm$ 7.28	33.63 $\pm$ 10.93	30.75 $\pm$ 7.54	1.865	0.160
Gender (M/F)	20/12	18/12	18/14	0.263	0.877
Education, years	13.55 $\pm$ 3.51	12.57 $\pm$ 2.91	13.50 $\pm$ 3.57	1.125	0.329
<i>Clinical measures</i>					
Y-BOCS total	26.59 $\pm$ 4.89	0.83 $\pm$ 1.53	1.41 $\pm$ 2.42	662.875	<0.001
Y-BOCS obsession	15.31 $\pm$ 2.93	0.33 $\pm$ 0.84	1.00 $\pm$ 1.72	523.984	<0.001
Y-BOCS compulsion	11.28 $\pm$ 4.86	0.50 $\pm$ 1.07	0.41 $\pm$ 1.04	162.272	<0.001
OCI-R	23.62 $\pm$ 13.22	7.97 $\pm$ 8.86	15.37 $\pm$ 13.50	13.501	<0.001
STAI state	53.16 $\pm$ 16.96	24.40 $\pm$ 17.63	39.00 $\pm$ 12.79	15.979	<0.001
STAI trait	53.34 $\pm$ 15.10	23.73 $\pm$ 17.93	40.81 $\pm$ 13.14	18.214	<0.001
BDI	18.06 $\pm$ 11.44	2.50 $\pm$ 5.24	8.81 $\pm$ 9.64	19.209	<0.001

#### 3.3. Relationship between connection strength and clinical variables in OCD patients

None of the correlation analysis between connection strength and OCD symptoms revealed a significant correlation, controlling for age, gender, years of education, BDI, SAT scores and disease duration (Fig. 2).

#### 3.4. Relationship between connection strength and symptom or diagnosis

We next regressed the strength of rich club, feeder, and local connections on OCD diagnosis, symptoms and covariates, across all subjects. We first tested Model 1: rich club connection strength  $\sim$  OCD diagnosis + compulsion symptom + covariates. This analysis revealed an association between diagnosis and rich club connection strength ( $\beta$ [SE] =  $-248.5874$ [138.257];  $p = 0.076$ ), while the association with compulsion or obsession scores and rich club connection strength ( $\beta$ [SE] =  $5.446$ [10.351];  $p = 0.600$ ) was much smaller (Fig. 3, left). In Model 2: rich club connection strength  $\sim$  OCD diagnosis + obsession symptom + covariates, no significant relationship was found.

In Model 3: feeder connection strength  $\sim$  OCD diagnosis + obsession symptom + covariates, no significant relationship was found. Next, Model 4: feeder connection strength  $\sim$  OCD diagnosis + compulsion symptom + covariates, revealed a significant relationship between diagnosis and feeder connection strength ( $\beta$ [SE] =  $-669.4794$ [264.577];  $p = 0.013$ ), while the association with compulsion or obsession scores and feeder connection strength ( $\beta$ [SE] =  $12.213$ [19.808];  $p = 0.539$ ) was much smaller (Fig. 3, middle).

Model 5: local connection strength  $\sim$  OCD diagnosis + compulsion symptom + covariates, revealed a significant association between diagnosis and local connection strength ( $\beta$ [SE] =  $-1340.172$ [528.165];  $p = 0.013$ ), while the association with compulsion or obsession scores and local connection strength ( $\beta$ [SE] =  $10.628$ [39.542];  $p = 0.789$ ) was much smaller (Fig. 3, right). Finally, in Model 6: local connection strength  $\sim$  OCD diagnosis + obsession symptom + covariates, no significant relationship was found.

#### 3.5. SC-FC coupling

There is no significant difference on whole-brain SC-FC coupling observed between healthy controls ( $r_{\text{mean}} = 0.168$ ), OCD patients ( $r_{\text{mean}} = 0.173$ ) and their unaffected first-degree relatives ( $r_{\text{mean}} = 0.148$ , Fig. 4). The SC-FC coupling for the rich club network was higher in healthy controls ( $r_{\text{mean}} = 0.346$ ) relative to the rich club coupling value in FDR ( $r_{\text{mean}} = 0.233$ ;  $p = 0.001$ ). In addition, no significant difference in SC-FC coupling was found in the feeder and local connection.

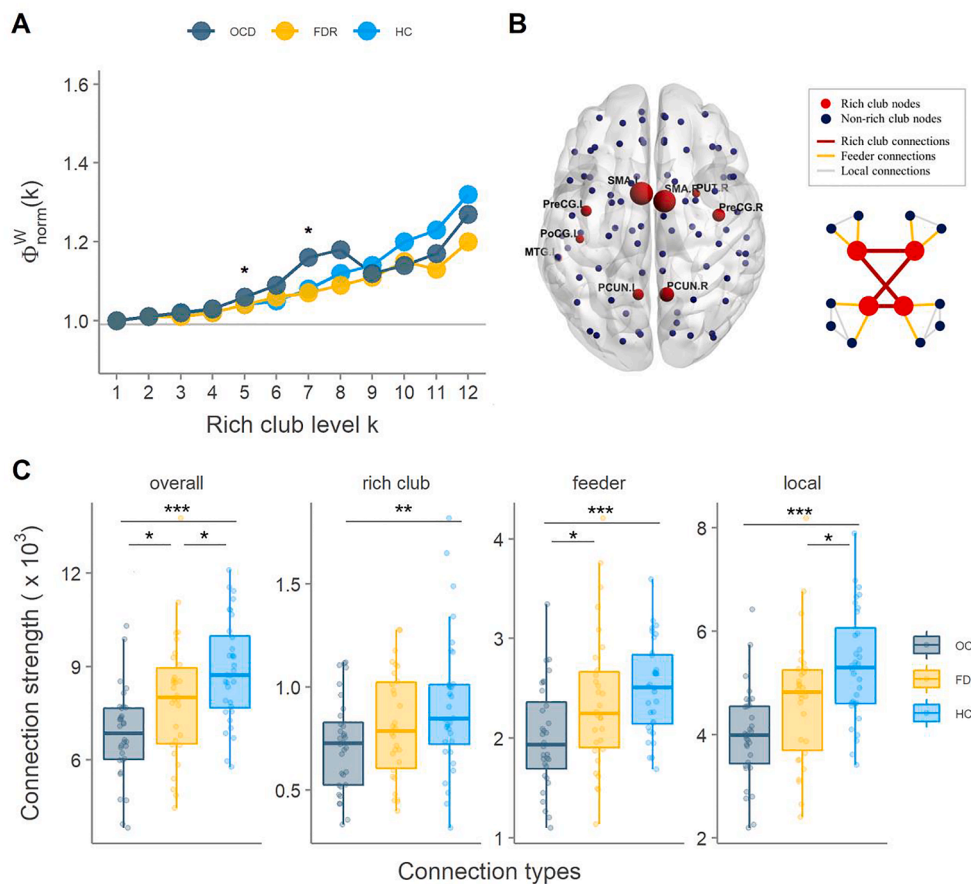


**Fig. 1.** Rich club organization. (A): The mean normalized rich club coefficient curve under a series of thresholds  $k$  for each group. (B): Rich-club regions in OCD, FDR, and HC groups. (C): Group differences in the connection strength of the overall, rich club, feeder, and local connections. PUT: putamen; PreCG: precentral gyrus; PCUN: precuneus; SMA: supplementary motor area; PoCG: postcentral gyrus; MTC: temporal middle gyrus. L: left; R: right. \*:  $p < 0.05$ , \*\*:  $p < 0.01$ , \*\*\*:  $p < 0.001$ .

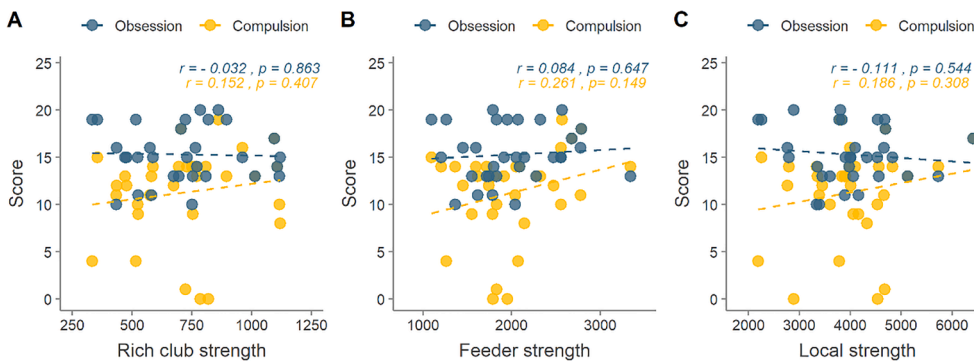


**Fig. 2.** The association of Y-BOCS compulsion or obsession with rich club connections, feeder connections, and local connections in OCD patients. (A): Association between rich club connection strength and compulsion and obsession score in patients. (B): Same correlations for feeder strength and (C) for local connection strength. Compulsion and obsession were measured with Y-BOCS score.

#### 4. Discussion

Our study is the first to investigate structural rich club organization characteristics in OCD patients and their unaffected FDR using DTI technology, and relate it to functional connectivity. Compared with HC, rich-club connection strength showed a significant decrease in OCD patients, suggesting that a damaged rich club connection may be a core aspect of OCD. Additionally, in all subjects, when obsessive-compulsive symptoms and diagnosis were combined in the same analysis, a significant effect of diagnosis on peripheral connections (i.e. feeder, and local connection strength) was observed. Our findings suggested that OCD

patients are characterized by a damaged rich-club backbone and degenerative peripheral (feeder and local) connections, which may be vulnerability factors for OCD. Finally, the decreased SC-FC rich club coupling coefficients in FDR compared to HC, provided further multimodal neuroimaging evidence for the role of rich-club connectivity in OCD.

The rich club regions were observed both in OCD patients, FDR and HC in this study, comprising the right putamen, bilateral precentral gyrus, left temporal middle gyrus, bilateral precuneus, left postcentral gyrus, and bilateral supplementary motor area. Our finding of rich club regions is to a large extent consistent with previous research on whole-

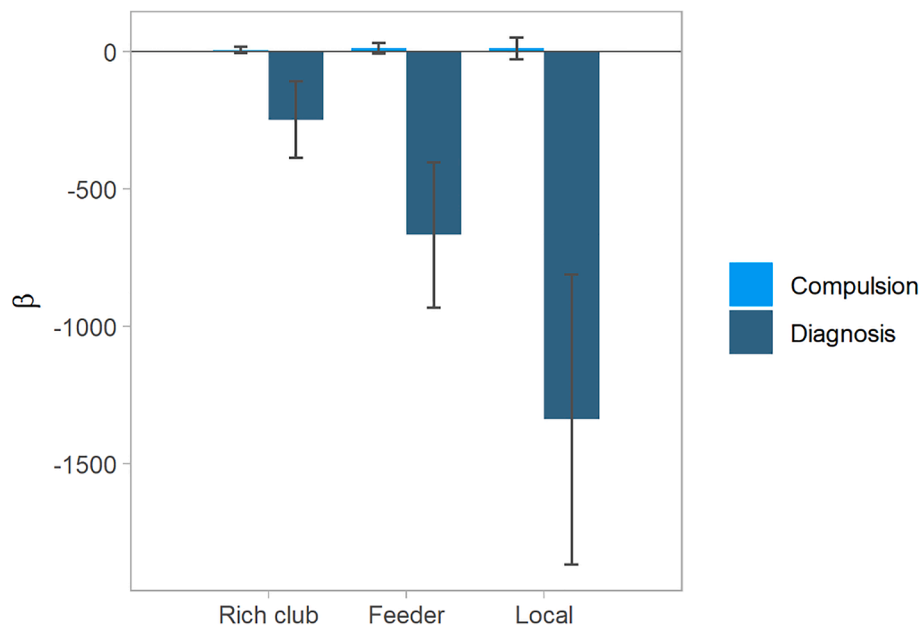


Fig. 3. The regression analysis comparing the predicting effects of OCD diagnosis with compulsion on connection strength. Model 1 (on the left), Model 4 (middle), and Model 5 (right). Error bars indicate SEs.

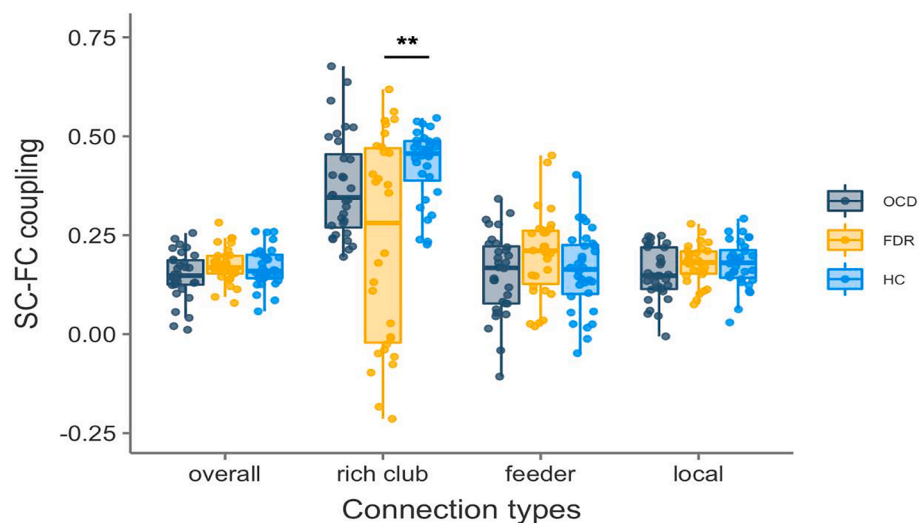


Fig. 4. Group comparisons in SC-FC coupling of three types of connections. (A): Group differences in SC-FC coupling of all connections were included. (B): SC-FC coupling of rich club connection, (C): of feeder connection and (D): local connection. \*\*:  $p < 0.01$ .

brain structural networks in OCD (Zhou et al., 2020). Additionally, the putamen and precentral gyrus were also found to be important hubs in the present study; these regions were also associated with OCD pathomechanism, including in the cortico-striatal circuits in previous studies (Jang et al., 2010; Kubota et al., 2019; Rasgon et al., 2017; Zhou et al., 2020). Moreover, these rich club nodes overlapped with the default mode network (DMN). Previous studies have revealed a disrupted connectivity of the DMN including the insula, superior parietal, and temporal cortex in OCD (Peng et al., 2014b).

The connections among the rich club regions contribute to highly efficient information integration due to their central position in the network topology (van den Heuvel and Sporns, 2011; van den Heuvel et al., 2013). In the present study, we found decreased rich club connection strength in OCD patients and FDR relative to HC, indicating abnormal connectivity in rich club regions. The abnormal rich club connectivity in patients suggests decreased brain communication and

integration in OCD. Our current findings are inconsistent with previous research on rich club organization of OCD (Zhou et al., 2020), which reported increased rich club, feeder and local connection strength in OCD patients. We observed a decreased structural rich club, local and feeder connectivity in OCD patients relative to HC. On the one hand, these differences may be caused by the heterogeneity of patients, the diversity in technical methods, and the inclusion of an FDR group. On the other hand, different network construction methods and parameters may lead to different results: This remains to be tested in future work.

Another noteworthy finding was that the SC-FC coupling of rich club connections in FDR was significantly decreased compared to HC. Interestingly, the decrease of the coupling coefficient in FDR was significant, although in OCD it was non-significantly decreased compared with HC, possibly as a reflection of the increased dynamics between structural and functional connection in FDR (van den Heuvel et al., 2013). Combined with the results of ordered differences in overall

strength (i.e.  $HC > FDR > OCD$ ), we tentatively conclude that the brain networks of the patients and their relatives are partially impaired in information communication, and the decreased SC-FC coupling of FDR may be a buffering mechanism for OCD. However, an important caveat is in order here, since whether this coupling is temporary or persistent cannot be identified in present design, and thus awaits future research for clarification.

Detecting abnormalities on unaffected FDR of OCD patients provides abundant information for OCD study, free of the effects of psychosis and antipsychotic medication (Peng et al., 2013). Currently, for the FDR, we identified a similar trend of changes in rich club and peripheral connection strength to OCD patients and ordered differences between patients and healthy subjects such that  $HC > FDR > OCD$ , reflecting a possible vulnerability biomarker for OCD. Our findings provided powerful evidence for changed whole-brain network properties in OCD patients. Moreover, our study presented a stronger relationship between peripheral connections and OCD diagnosis labels but not between rich club connections and symptoms, which suggests that OCD diagnosis can capture the alteration in peripheral connections in contrast to symptoms. The abnormalities in rich club and peripheral networks we found seem to indicate that dysconnectivity includes a neurodevelopmental vulnerability to the disease, which may be mediated by genetic factors (Collin et al., 2014).

The severity of obsessive or compulsive symptoms do not meet the diagnosis criteria in healthy persons who are genetically related to patients (e.g., FDR). Yet, the imperceptible alterations in brain structure may occur much earlier (Fan et al., 2016). We also observed alterations of peripheral connections in the FDR group. Given the relatively small effect size and cross-sectional nature of our study, however, the relation between local network properties and symptom or diagnosis should be regarded as preliminary.

Our research has some limitations. First, due to the inherent limitation of the deterministic tracking method, accurately reconstructing the cross-fibers in the human brain was difficult. In future work, probabilistic tractography could be used for supplementary verification. Second, the sample size of our study was not large, and drug-taking patients were also recruited. Third, anxiety and depression scores in HC were higher than FDR, which may stem from the fact that the healthy subjects were college students with high academic stress. A larger sample size, balanced parameters and controlled medication patients should be employed in the future to mitigate these limitations. Finally, longitudinal and developmental studies are required to uncover the causal relationship between structural and functional connectivity on the one hand, and OCD presence and symptomatology on the other.

## 5. Conclusion

We examined the rich club organization in OCD patients and their unaffected first-degree relatives with deterministic tractography and functional connectivity methods. The damaged rich club organization and decreased connectivity of peripheral nodes in OCD patients and FDR may suggest functional deficits in brain networks of OCD. Moreover, our finding revealed an alteration in OCD and their FDR, supporting the idea that altered rich club organization is related to a familial vulnerability to OCD, potentially representing a vulnerability biomarker of the disorder.

## CRediT authorship contribution statement

**Ziwen Peng:** Conceptualization, Methodology, Writing - original draft. **Xinyi Yang:** Data curation, Formal analysis, Writing - original draft. **Chuanyong Xu:** Data curation, Software, Writing - original draft. **Xiangshu Wu:** Data curation, Visualization. **Qiong Yang:** Project administration. **Zhen Wei:** Investigation. **Zihan Zhou:** Investigation. **Tom Verguts:** Writing - review & editing. **Qi Chen:** Supervision, Writing - review & editing.

## Declaration of Competing Interest

The authors declare that they have no known competing financial interests or personal relationships that could have appeared to influence the work reported in this paper.

## Acknowledgment

This study was partly supported by National Natural Science Foundation of China (31871113, 31920103009, 32071049, 31900770 and 31671135).

## Appendix A. Supplementary data

Supplementary data to this article can be found online at <https://doi.org/10.1016/j.nicl.2021.102808>.

## References

- Banks, G.P., Mikell, C.B., Youngerman, B.E., Henriques, B., Kelly, K.M., Chan, A.K., Herrera, D., Dougherty, D.D., Eskandar, E.N., Sheth, S.A., 2015. Neuroanatomical Characteristics Associated With Response to Dorsal Anterior Cingulotomy for Obsessive-Compulsive Disorder. *JAMA Psychiatry* 72 (2), 127. <https://doi.org/10.1001/jamapsychiatry.2014.2216>.
- Beck, A.T., Steer, R.A., 1984. Internal consistencies of the original and revised beck depression inventory. 40(6), 1365-1367. 10.1002/1097-4679(198411)40:6<1365::Aid-jclp2270400615>3.0.Co;2-d.
- Bullmore, E., Sporns, O., 2009. Complex brain networks: graph theoretical analysis of structural and functional systems. *Nat. Rev. Neurosci.* 10 (3), 186–198. <https://doi.org/10.1038/nrn2575>.
- Cao, R., Wang, X., Gao, Y., Li, T., Zhang, H., Hussain, W., et al., 2020. Abnormal Anatomical Rich-Club Organization and Structural-Functional Coupling in Mild Cognitive Impairment and Alzheimer's Disease. 11(53). 10.3389/fneur.2020.00053.
- Chamberlain, S.R., Menzies, L., Hampshire, A., Suckling, J., Fineberg, N.A., del Campo, N., Aitken, M., Craig, K., Owen, A.M., Bullmore, E.T., Robbins, T.W., Sahakian, B.J., 2008. Orbitofrontal Dysfunction in Patients with Obsessive-Compulsive Disorder and Their Unaffected Relatives. *Science (New York)* 321 (5887), 421–422. <https://doi.org/10.1126/science.1154433>.
- Colizza, V., Flammini, A., Serrano, M.A., Vespignani, A., 2006. Detecting rich-club ordering in complex networks. *Nat. Phys.* 2 (2), 110–115. <https://doi.org/10.1038/nphys209>.
- Collin, G., Kahn, R.S., de Reus, M.A., Cahn, W., van den Heuvel, M.P., 2014. Impaired Rich Club Connectivity in Unaffected Siblings of Schizophrenia Patients. *Schizophr. Bull.* 40 (2), 438–448. <https://doi.org/10.1093/schbul/sbt162>.
- Cui, G., Ou, Y., Chen, Y., Lv, D., Jia, C., Zhong, Z., et al., 2020. Altered Global Brain Functional Connectivity in Drug-Naive Patients With Obsessive-Compulsive Disorder. 11(98). 10.3389/fpsy.2020.00098.
- Cui, Z., Zhong, S., Xu, P., Gong, G., He, Y., 2013. PANDA: a pipeline toolbox for analyzing brain diffusion images. *Front. Hum. Neurosci.* 7, 42.
- Dikmeer, N., Besiroglu, L., Di Biase, M.A., Zalesky, A., Kasal, M.L., Bilge, A., Durmaz, E., Polat, S., Gelal, F., Zorlu, N., 2021. White matter microstructure and connectivity in patients with obsessive-compulsive disorder and their unaffected siblings. *Acta Psychiatr. Scand.* 143 (1), 72–81. <https://doi.org/10.1111/acps.v143.110.1111/acps.13241>.
- Fajnerova, I., Gregus, D., Francova, A., Noskova, E., Koprivova, J., Stopkova, P., et al., 2020. Functional Connectivity Changes in Obsessive-Compulsive Disorder Correspond to Interference Control and Obsessions Severity. 11(568). 10.3389/fneur.2020.00568.
- Fan, S., van den Heuvel, O.A., Cath, D.C., van der Werf, Y.D., de Wit, S.J., de Vries, F.E., Veltman, D.J., Pouwels, P.J.W., 2016. Mild white matter changes in un-medicated obsessive-compulsive disorder patients and their unaffected siblings. *Front. Neurosci.* 9 <https://doi.org/10.3389/fnins.2015.00495>.
- First, M., Spitzer, R.L., Gibbon, M.L., Williams, J., 2002. Structured clinical interview for DSM-IV-TR Axis I Disorders. Research Version, Non-patient Edition.
- Friston, K.J., Williams, S., Howard, R., Frackowiak, R.S.J., Turner, R., 1996. Movement-related effects in fMRI time-series. *Magn. Reson. Med.* 35 (3), 346–355. <https://doi.org/10.1002/mrm.1910350312>.
- Goodman, W.K., Price, L.H., Rasmussen, S.A., Mazure, C., Fleischmann, R.L., Hill, C.L., et al., 1989. The Yale-Brown Obsessive Compulsive Scale: I. Development, Use, and Reliability. *Arch. Gen. Psychiatry* 46 (11), 1006–1011. <https://doi.org/10.1001/archpsyc.1989.01810110048007>.
- Greicius, M.D., Supekar, K., Menon, V., Dougherty, R.F., 2009. Resting-State Functional Connectivity Reflects Structural Connectivity in the Default Mode Network. *Cereb. Cortex* 19 (1), 72–78. <https://doi.org/10.1093/cercor/bhn059>.
- Hanna, G.L., Veenstra-VanderWeele, J., Cox, N.J., Boehnke, M., Himle, J.A., Curtis, G.C., Leventhal, B.L., Cook, E.H., 2002. Genome-wide linkage analysis of families with obsessive-compulsive disorder ascertained through pediatric probands. *Am. J. Med. Genet.* 114 (5), 541–552. <https://doi.org/10.1002/ajmg.v114:510.1002/ajmg.10519>.

- Honey, C.J., Sporns, O., Cammoun, L., Gigandet, X., Thiran, J.P., Meuli, R., Hagmann, P., 2009. Predicting human resting-state functional connectivity from structural connectivity. *Proc. Natl. Acad. Sci.* 106 (6), 2035–2040. <https://doi.org/10.1073/pnas.0811168106>.
- Hu, X., Zhang, L., Bu, X., Li, H., Gao, Y., Lu, L.u., Tang, S., Wang, Y., Huang, X., Gong, Q., 2020. White matter disruption in obsessive-compulsive disorder revealed by meta-analysis of tract-based spatial statistics. *Depression Anxiety* 37 (7), 620–631. <https://doi.org/10.1002/da.v37.7.10.1002/da.23008>.
- Irimia, A., Chambers, M.C., Torgerson, C.M., Van Horn, J.D., 2012. Circular representation of human cortical networks for subject and population-level connectomic visualization. *NeuroImage* 60 (2), 1340–1351. <https://doi.org/10.1016/j.neuroimage.2012.01.107>.
- Jang, J.H., Kim, J.-H., Jung, W.H., Choi, J.-S., Jung, M.H., Lee, J.-M., Choi, C.-H., Kang, D.-H., Kwon, J.S., 2010. Functional connectivity in fronto-subcortical circuitry during the resting state in obsessive-compulsive disorder. *Neurosci. Lett.* 474 (3), 158–162. <https://doi.org/10.1016/j.neulet.2010.03.031>.
- Jbabdi, S., Sotiropoulos, S.N., Haber, S.N., Van Essen, D.C., Behrens, T.E., 2015. Measuring macroscopic brain connections in vivo. *Nat. Neurosci.* 18 (11), 1546–1555. <https://doi.org/10.1038/nn.4134>.
- Koh, Y.H., Shih, Y.-C., Lim, S.L., Kiew, Y.S., Lim, E.W., Ng, S.M., Ooi, L.Q.R., Tan, W.Q., Chung, Y.-C., Rumpel, H., Tan, E.K., Chan, L.L., 2020. Evaluation of trigeminal nerve tractography using two-fold-accelerated simultaneous multi-slice readout-segmented echo planar diffusion tensor imaging. *Eur. Radiol.* 31 (2), 640–649. <https://doi.org/10.1007/s00330-020-07193-x>.
- Kubota, Y., Sato, W., Kochiyama, T., Uono, S., Yoshimura, S., Sawada, R., Toichi, M., 2019. Corticostriatal-limbic correlates of sub-clinical obsessive-compulsive traits. *Psychiatry Res.* 285, 40–46. <https://doi.org/10.1016/j.psychres.2019.01.012>.
- Lee, W.J., Han, C.E., Aganj, I., Seo, S.W., Seong, J.-K., Adamson, M., 2018. Distinct Patterns of Rich Club Organization in Alzheimer's Disease and Subcortical Vascular Dementia: A White Matter Network Study. *J. Alzheimers Dis.* 63 (3), 977–987. <https://doi.org/10.3233/JAD-180027>.
- Li, D., Cui, X., Yan, T., Liu, B.o., Zhang, H., Xiang, J., Wang, B., 2019. Abnormal Rich Club Organization in Hemispheric White Matter Networks of ADHD. *J. Attention Disorders* 25 (9), 1215–1229. <https://doi.org/10.1177/1087054719892887>.
- Li, Z., Peck, K.K., Brennan, N.P., Jenabi, M., Hsu, M., Zhang, Z., Holodny, A.I., Young, R. J., 2013. Diffusion tensor tractography of the arcuate fasciculus in patients with brain tumors: Comparison between deterministic and probabilistic models. *J. Biomed. Sci. Eng.* 06 (02), 192–200. <https://doi.org/10.4236/jbise.2013.62023>.
- Liu, X., He, C., Fan, D., Zhu, Y., Zang, F., Wang, Q., Zhang, H., Zhang, Z., Zhang, H., Xie, C., 2020. Disrupted rich-club network organization and individualized identification of patients with major depressive disorder. *Prog. Neuro-Psychopharmacol. Biol. Psychiatry* 108, 110074. <https://doi.org/10.1016/j.pnpbp.2020.110074>.
- Menzies, L., Williams, G.B., Chamberlain, S.R., Ooi, C., Fineberg, N., Suckling, J., Sahakian, B.J., Robbins, T.W., Bullmore, E.T., 2008. White Matter Abnormalities in Patients With Obsessive-Compulsive Disorder and Their First-Degree Relatives. *Am. J. Psychiatry* 165 (10), 1308–1315. <https://doi.org/10.1176/appi.ajp.2008.07101677>.
- Mori, S., Crain, B.J., Chacko, V.P., Van Zijl, P.C.M., 1999. Three-dimensional tracking of axonal projections in the brain by magnetic resonance imaging. *Ann. Neurol.* 45 (2), 265–269. [https://doi.org/10.1002/\(ISSN\)1531-8249](https://doi.org/10.1002/(ISSN)1531-8249).
- Nestadt, G., Samuels, J., Riddle, M., Bienvenu, O.J., Liang, K.-Y., LaBuda, M., Walkup, J., Grados, M., Hoehn-Saric, R., 2000. A Family Study of Obsessive-compulsive Disorder. *Arch. Gen. Psychiatry* 57 (4), 358. <https://doi.org/10.1001/archpsyc.57.4.358>.
- Pauls, David, L., Alsbrook, II, John, et al., 1995. A family study of obsessive-compulsive disorder. *152(1)*, 76–84. <https://doi.org/10.1176/ajp.152.1.76>.
- Peng, Z., Yang, W., Miao, G., Jing, J., Chan, R.C.K., 2011. The Chinese version of the Obsessive-Compulsive Inventory-Revised scale: Replication and extension to non-clinical and clinical individuals with OCD symptoms. *BMC Psychiatry* 11 (1), 129. <https://doi.org/10.1186/1471-244X-11-129>.
- Peng, Z., Shi, F., Shi, C., Miao, G., Yang, Q., Gao, W., Wolff, J.J., Chan, R.C.K., Shen, D., Kassubek, J., 2014a. Structural and Diffusion Property Alterations in Unaffected Siblings of Patients with Obsessive-Compulsive Disorder. *PLoS ONE* 9 (1), e85663. <https://doi.org/10.1371/journal.pone.0085663>.
- Peng, Z., Shi, F., Shi, C., Yang, Q., Chan, R.C.K., Shen, D., 2013. Disrupted cortical network as a vulnerability marker for obsessive-compulsive disorder. *Brain Struct. Funct.* 219 (5), 1801–1812. <https://doi.org/10.1007/s00429-013-0602-y>.
- Peng, Z.W., Xu, T., He, Q.H., Shi, C.Z., Wei, Z., Miao, G.D., Jing, J., Lim, K.O., Zuo, X.N., Chan, R.C.K., 2014b. Default network connectivity as a vulnerability marker for obsessive compulsive disorder. *Psychol. Med.* 44 (7), 1475–1484. <https://doi.org/10.1017/S0033291713002250>.
- Power, J.D., Barnes, K.A., Snyder, A.Z., Schlaggar, B.L., Petersen, S.E., 2012. Spurious but systematic correlations in functional connectivity MRI networks arise from subject motion. *NeuroImage* 59 (3), 2142–2154. <https://doi.org/10.1016/j.neuroimage.2011.10.018>.
- Rasgon, A., Lee, W.H., Leib, E., Laird, A., Glahn, D., Goodman, W., Frangou, S., 2017. Neural correlates of affective and non-affective cognition in obsessive compulsive disorder: A meta-analysis of functional imaging studies. *European Psychiatry* 46, 25–32. <https://doi.org/10.1016/j.eurpsy.2017.08.001>.
- Reess, T.J., Rus, O.G., Schmidt, R., de Reus, M.A., Zaudig, M., Wagner, G., Zimmer, C., van den Heuvel, M.P., Koch, K., 2016. Connectomics-based structural network alterations in obsessive-compulsive disorder. *Transl. Psychiatry* 6 (9), e882. <https://doi.org/10.1038/tp.2016.163>.
- Robbins, T.W., Vaghi, M.M., Banca, P., 2019. Obsessive-Compulsive Disorder: Puzzles and Prospects. *Neuron* 102 (1), 27–47. <https://doi.org/10.1016/j.neuron.2019.01.046>.
- Rubinov, M., Sporns, O., 2010. Complex network measures of brain connectivity: Uses and interpretations. *NeuroImage* 52 (3), 1059–1069. <https://doi.org/10.1016/j.neuroimage.2009.10.003>.
- Sa de Almeida, J., Meskaldji, D.-E., Loukas, S., Lordier, L., Gui, L., Lazeyras, F., Hüppi, P. S., 2021. Preterm birth leads to impaired rich-club organization and fronto-paralimbic/limbic structural connectivity in newborns. *NeuroImage* 225, 117440. <https://doi.org/10.1016/j.neuroimage.2020.117440>.
- Smith, S.M., Jenkinson, M., Woolrich, M.W., Beckmann, C.F., Behrens, T.E.J., Johansen-Berg, H., Bannister, P.R., De Luca, M., Drobnjak, I., Flitney, D.E., Niazy, R.K., Saunders, J., Vickers, J., Zhang, Y., De Stefano, N., Brady, J.M., Matthews, P.M., 2004. Advances in functional and structural MR image analysis and implementation as FSL. *NeuroImage* 23, S208–S219. <https://doi.org/10.1016/j.neuroimage.2004.07.051>.
- Spielberger, C.D., 1983. *State-trait anxiety inventory (STAI)*. *Mind Gard.* 94061, 261–3500.
- Sporns, O., 2011. The human connectome: a complex network. *Ann. N. Y. Acad. Sci.* 1224, 109–125. <https://doi.org/10.1111/j.1749-6632.2010.05888.x>.
- Sporns, O., Honey, C.J., Kötter, R., Kaiser, M., 2007. Identification and Classification of Hubs in Brain Networks. *PLoS ONE* 2 (10), e1049. <https://doi.org/10.1371/journal.pone.0001049>.
- Sporns, O., Tononi, G., Kötter, R., 2005. The Human Connectome: A Structural Description of the Human Brain. *PLoS Comput. Biol.* 1 (4), e42. <https://doi.org/10.1371/journal.pcbi.0010042>.
- Stern, E.R., Fitzgerald, K.D., Welsh, R.C., Abelson, J.L., Taylor, S.F., Soriano-Mas, C., 2012. Resting-State Functional Connectivity between Fronto-Parietal and Default Mode Networks in Obsessive-Compulsive Disorder. *PLoS ONE* 7 (5), e36356. <https://doi.org/10.1371/journal.pone.0036356>.
- Tuladhar, A.M., Lawrence, A., Norris, D.G., Barrick, T.R., Markus, H.S., de Leeuw, F.-E., 2017. Disruption of rich club organisation in cerebral small vessel disease. *Human Brain Mapping* 38 (4), 1751–1766. <https://doi.org/10.1002/hbm.23479>.
- Tzourio-Mazoyer, N., Landeau, B., Papathanassiou, D., Crivello, F., Etard, O., Delcroix, N., Mazoyer, B., Joliot, M., 2002. Automated Anatomical Labeling of Activations in SPM Using a Macroscopic Anatomical Parcellation of the MNI MRI Single-Subject Brain. *NeuroImage* 15 (1), 273–289. <https://doi.org/10.1006/nimg.2001.0978>.
- Vaghi, M.M., Hampshire, A., Fineberg, N.A., Kaser, M., Briühl, A.B., Sahakian, B.J., et al., 2017. Hypoactivation and Dysconnectivity of a Fronto-striatal Circuit During Goal-Directed Planning as an Endophenotype for Obsessive-Compulsive Disorder. *Biol. Psychiatry* 2 (8), 655–663. <https://doi.org/10.1016/j.bpsc.2017.05.005>.
- van den Heuvel, M.P., Mandl, R.C.W., Stam, C.J., Kahn, R.S., Hulshoff Pol, H.E., 2010. Aberrant Frontal and Temporal Complex Network Structure in Schizophrenia: A Graph Theoretical Analysis. *J. Neurosci.* 30 (47), 15915. <https://doi.org/10.1523/JNEUROSCI.2874-10.2010>.
- van den Heuvel, M.P., Sporns, O., 2011. Rich-Club Organization of the Human Connectome. *J. Neurosci.* 31 (44), 15775. <https://doi.org/10.1523/JNEUROSCI.3539-11.2011>.
- van den Heuvel, M.P., Sporns, O., Collin, G., Scheewe, T., Mandl, R.C.W., Cahn, W., et al., 2013. Abnormal Rich Club Organization and Functional Brain Dynamics in Schizophrenia. *JAMA Psychiatry* 70 (8), 783–792. <https://doi.org/10.1001/jamapsychiatry.2013.1328> %J *JAMA Psychiatry*.
- Wang, B., Wang, X., Cao, R., Xiang, J., Yan, T., et al., 2019. Rich-Club Analysis in Adults With ADHD Connectomes Reveals an Abnormal Structural Core Network. *J. Attention Disorders* 1087054719883031. <https://doi.org/10.1177/1087054719883031>.
- Wang, J., Wang, X., Xia, M., Liao, X., Evans, A., He, Y., 2015. GREYNA: a graph theoretical network analysis toolbox for imaging connectomics. *Front. Hum. Neurosci.* 9, 386. <https://doi.org/10.3389/fnhum.2015.00386>.
- Wang, R., Benner, T., Sorensen, A., Wedeen, V.J., 2007. Diffusion Toolkit: A Software Package for Diffusion Imaging Data Processing and Tractography. *Proc Intl Soc Mag Reson Med* 15.
- Wang, Y., Deng, F., Jia, Y., Wang, J., Zhong, S., Huang, H., et al., 2018. Disrupted rich club organization and structural brain connectome in unmedicated bipolar disorder. *Psychol. Med.* 49 (3), 510–518. <https://doi.org/10.1017/S0033291718001150>.
- Wang, Z., Dai, Z., Gong, G., Zhou, C., He, Y., 2014. Understanding Structural-Functional Relationships in the Human Brain: A Large-Scale Network Perspective. *Neuroscientist* 21 (3), 290–305. <https://doi.org/10.1177/1073858414537560>.
- Xia, M., Wang, J., He, Y., 2013. BrainNet Viewer: A Network Visualization Tool for Human Brain Connectomics. *PLoS ONE* 8 (7), e68910. <https://doi.org/10.1371/journal.pone.0068910>.
- Yan, C.-G., Wang, X.-D., Zuo, X.-N., Zang, Y.-F., 2016. DPABI: Data Processing & Analysis for (Resting-State) Brain Imaging. *Neuroinformatics* 14 (3), 339–351. <https://doi.org/10.1007/s12021-016-9299-4>.
- Yan, T., Wang, W., Yang, L., Chen, K., Chen, R., Han, Y., 2018. Rich club disturbances of the human connectome from subjective cognitive decline to Alzheimer. *Theranostics* 8 (12), 3237–3255. <https://doi.org/10.7150/thno.23772>.
- Zhang, R., Shao, R., Guiyun, X., Lu, W., Zheng, W., Miao, Q., et al., 2018. Aberrant Brain Structural-Functional Connectivity Coupling in Euthymic Bipolar Disorder. *Hum. Brain Mapp.* 40 (12), 3452–3463. <https://doi.org/10.1002/hbm.23448>.



- Zhang, T., Wang, J., Yang, Y., Wu, Q., Li, B., Chen, L., et al., 2011a. Abnormal small-world architecture of top-down control networks in obsessive-compulsive disorder. *J. Psychiatry Neurosci.* 36 (1), 23–31. <https://doi.org/10.1503/jpn.100006>.
- Zhang, Z., Liao, W., Chen, H., Mantini, D., Ding, J.-R., Xu, Q., et al., 2011b. Altered functional–structural coupling of large-scale brain networks in idiopathic generalized epilepsy. *Brain* 134 (10), 2912–2928. <https://doi.org/10.1093/brain/awr223>.
- Zhou, C., Ping, L., Chen, W., He, M., Xu, J., Shen, Z., et al., 2020. Altered white matter structural networks in drug-naïve patients with obsessive-compulsive disorder. *Brain Imaging Behav.* <https://doi.org/10.1007/s11682-020-00278-7>.